11096 *Inorg. Chem.* **2010**, *49*, 11096–11105
DOI: 10.1021/ic101668f

Inorganic Chemistry
Article

Self-Assembled 3D Heterometallic Cu^{II}/Fe^{II} Coordination Polymers with Octahedral Net Skeletons: Structural Features, Molecular Magnetism, Thermal and Oxidation Catalytic Properties

Yauhen Y. Karabach,[†] M. Fátima C. Guedes da Silva,[†,‡] Maximilian N. Kopylovich,[†] Beatriz Gil-Hernández,[§] Joaquin Sanchiz,[§] Alexander M. Kirillov,*[,†] and Armando J. L. Pombeiro*[,†]

[†]*Centro de Química Estrutural, Complexo I, Instituto Superior Técnico, TU Lisbon, Av. Rovisco Pais, 1049-001, Lisbon, Portugal,* [‡]*Universidade Lusófona de Humanidades e Tecnologias, ULHT Lisbon, Av. do Campo Grande, 376, 1749-024, Lisbon, Portugal, and* [§]*Departamento de Química Inorgánica, Facultad de Química, Grupo de Materiales Magnéticos, Universidad de La Laguna, C. Astrofísico F. Sánchez, s/n, 38206, La Laguna, Tenerife, Spain*

Received August 17, 2010

The new three-dimensional (3D) heterometallic Cu^{II}/Fe^{II} coordination polymers $[Cu_6(H_2tea)_6Fe(CN)_6]_n(NO_3)_{2n}\cdot 6nH_2O$ (**1**) and $[Cu_6(Hmdea)_6Fe(CN)_6]_n(NO_3)_{2n}\cdot 7nH_2O$ (**2**) have been easily generated by aqueous-medium self-assembly reactions of copper(II) nitrate with triethanolamine or *N*-methyldiethanolamine (H_3tea or H_2mdea, respectively), in the presence of potassium ferricyanide and sodium hydroxide. They have been isolated as air-stable crystalline solids and fully characterized including by single-crystal X-ray diffraction analyses. The latter reveal the formation of 3D metal−organic frameworks that are constructed from the $[Cu_2(\mu\text{-}H_2tea)_2]^{2+}$ or $[Cu_2(\mu\text{-}Hmdea)_2]^{2+}$ nodes and the octahedral $[Fe(CN)_6]^{4-}$ linkers, featuring regular (**1**) or distorted (**2**) octahedral net skeletons. Upon dehydration, both compounds show reversible escape and binding processes toward water or methanol molecules. Magnetic susceptibility measurements of **1** and **2** reveal strong antiferromagnetic [$J = -199(1)$ cm^{-1}] or strong ferromagnetic [$J = +153(1)$ cm^{-1}] couplings between the copper(II) ions through the μ-O-alkoxo atoms in **1** or **2**, respectively. The differences in magnetic behavior are explained in terms of the dependence of the magnetic coupling constant on the Cu−O−Cu bridging angle. Compounds **1** and **2** also act as efficient catalyst precursors for the mild oxidation of cyclohexane by aqueous hydrogen peroxide to cyclohexanol and cyclohexanone (homogeneous catalytic system), leading to maximum total yields (based on cyclohexane) and turnover numbers (TONs) up to about 22% and 470, respectively.

Introduction

In recent years, the research on coordination polymers (and metal−organic frameworks) has attracted much interest in the areas of crystal engineering, inorganic, coordination, and materials chemistries, which is associated with the unusual structural diversity and important practical applications of such metal−organic materials.[1,2] Although great progress has been achieved in the synthesis and uses of homometallic coordination polymers, the polymeric networks that bear two different metals are less common,[3] being often composed of cyanometallate linkers.[3−5] These materials attract special attention because of potential synergic effects of different metals within one assembly, and a variety

*To whom correspondence should be addressed. E-mail: kirillov@ist.utl.pt (A.M.K.), pombeiro@ist.utl.pt (A.J.L.P.). Fax: +351 218464455.

(1) (a) Batten, S. R.; Turner, D. R.; Neville, S. M. *Coordination Polymers: Design, Analysis and Application*; Royal Society of Chemistry: London, 2009. (b) *Encyclopedia of Supramolecular Chemistry*; Atwood, J. L., Steed, J. W., Eds.; Taylor & Francis: London, 2004.

(2) For selected reviews, see: (a) Aakeröy, C. B.; Champness, N. R.; Janiak, C. *CrystEngComm* **2010**, *12*, 22. (b) Perry, J. J., IV; Perman, J. A.; Zaworotko, M. J. *Chem. Soc. Rev.* **2009**, *38*, 1400. (c) Robin, A. Y.; Fromm, K. M. *Coord. Chem. Rev.* **2006**, *250*, 2127. (d) Kitagawa, S.; Uemura, K. *Chem. Soc. Rev.* **2005**, *34*, 109. (e) Rao, C. N. R.; Natarajan, S.; Vaidhyanathan, R. *Angew. Chem., Int. Ed.* **2004**, *43*, 1466. (f) Kitagawa, S.; Kitaura, R.; Noro, S. *Angew. Chem., Int. Ed.* **2004**, *43*, 2334. (g) Janiak, C. *Dalton Trans.* **2003**, 2781. (h) James, S. L. *Chem. Soc. Rev.* **2003**, *32*, 276. (i) Moulton, B.; Zaworotko, M. *J. Chem. Rev.* **2001**, *101*, 1629.

(3) See the Cambridge Structural Database (CSD, version 5.31, May 2010): Allen, F. H. *Acta Crystallogr.* **2002**, *B58*, 380.

(4) For reviews on cyanometallate materials, see: (a) Sieklucka, B.; Podgajny, R.; Przychodzen, P.; Korzeniak, T. *Coord. Chem. Rev.* **2005**, *249*, 2203. (b) Rebilly, J.-N.; Mallah, T. *Struct. Bonding* (*Berlin*) **2006**, *122*, 103. (c) Miller, J. S.; Manson, J. L. *Acc. Chem. Res.* **2001**, *34*, 563.

(5) For reviews on the $[Fe(CN)_6]^{3-/4-}$ based materials, see: (a) Beltran, L. M. C.; Long, J. R. *Acc. Chem. Res.* **2005**, *38*, 325. (b) Ricci, F.; Palleschi, G. *Biosens. Bioelectron.* **2005**, *21*, 389. (c) de Tacconi, N. R.; Rajeshwar, K.; Lezna, R. O. *Chem. Mater.* **2003**, *15*, 3046. (d) Koncki, R. *Crit. Rev. Anal. Chem.* **2002**, *32*, 79. (e) Karyakin, A. A. *Electroanalysis* **2001**, *13*, 813.

 Published on Web 10/28/2010

of advanced applications (molecular magnets, electrodes, sensors, adsorbents, and gas storage systems).[4−6]

However, the majority of synthetic procedures for heterometallic coordination polymers is characterized by one or several of the following drawbacks: (i) involve complicated and multistep syntheses that may require inert atmosphere and air-sensitive chemicals, (ii) proceed in organic solvents or under hydrothermal conditions, (iii) require prior preparation of building blocks, often with costly ligands, and/or (iv) need precious metals.[1,2,4,6] In contrast, the engineering of heterometallic networks in aqueous medium, at ambient conditions, and using simple chemicals remains little explored. Hence, the development of such an approach constituted one of the main objectives of the present work.

Within our ongoing projects on aqueous-medium self-assembly syntheses of various coordination polymers[7] and/or multinuclear metal complexes,[8] we have recently reported a number of homometallic Cu or heterometallic Cu/Na metal−organic networks.[9] These compounds were easily constructed from various Cu-aminopolyalcoholate building blocks and aromatic polycarboxylate linkers, and show some notable structural, catalytic, magnetic, and host−guest features.[9] In pursuit of these studies, we have been interested in modifying both the synthetic strategy and the polymeric networks thereof, through the introduction of a metal-containing linker such as the hexacyanoferrate species, thus having an influence on the structural, magnetic, and catalytic properties of the resulting materials. The choice of $[Fe(CN)_6]^{3-/4-}$ is governed by its low cost, stability, solubility in water, availability of up to six coordinating moieties, and a recognized use[5,6,10] as a short-distance octahedral linker in the design of coordination networks. Besides, to our knowledge,[3] heterometallic Cu/Fe coordination polymers bearing Cu-aminopolyalcoholate nodes and hexacyanoferrate linkers are unknown. Moreover, the application of Cu/Fe framework materials in catalysis[11] also remains an underexplored area of research.

In the present study, we report a facile self-assembly route for the two new heterometallic Cu^{II}/Fe^{II} coordination polymers $[Cu_6(H_2tea)_6Fe(CN)_6]_n(NO_3)_{2n}\cdot 6nH_2O$ (**1**) and $[Cu_6(Hmdea)_6Fe(CN)_6]_n(NO_3)_{2n}\cdot 7nH_2O$ (**2**), which are readily formed by self-assembly of simple chemicals in aqueous media. These products have been fully characterized including by single-crystal X-ray diffraction analysis, and possess either regular (**1**) or distorted (**2**) three-dimensional (3D) octahedral net skeletons. The variable-temperature magnetic susceptibility behavior and thermal properties of **1** and **2** have been also studied. In addition, both compounds act as valuable catalyst precursors for the mild peroxidative oxidation of cyclohexane to cyclohexanol and cyclohexanone.

Experimental Section

Materials and Methods. All synthetic work was performed in air and at room temperature (ca. 25 °C). All chemicals were obtained from commercial sources and used as received. C, H, and N elemental analyses were carried out by the Microanalytical Service of the Instituto Superior Técnico. Infrared spectra (4000−400 cm^{-1}) were recorded on a BIO-RAD FTS 3000MX instrument in KBr pellets (abbreviations: vs - very strong, s - strong, m − medium, w − weak, br. − broad). Differential thermal analyses were performed with a Perkin-Elmer STA 6000 instrument. The crystalline samples (ca. 10 mg) were heated under N_2 atmosphere at the rate of 10 °C/min in the 30−750 °C temperature range. Magnetic susceptibility measurements on polycrystalline samples were carried out in the 2.0−300 K temperature range by means of a Quantum Design SQUID magnetometer operating with an applied magnetic field of 10.000 Oe. Diamagnetic corrections of the constituent atoms were estimated from Pascal's constants. Experimental susceptibilities were also corrected for the temperature-independent paramagnetism [60×10^{-6} cm^3 mol^{-1} *per* Cu(II)] and the magnetization of the sample holder.

General Synthetic Procedure for 1 and 2. To an aqueous solution (10.0 mL) containing $Cu(NO_3)_2\cdot 2.5H_2O$ (1.00 mmol, 233 mg) and HNO_3 (0.1 M, 1.00 mmol) [the acid was introduced to avoid spontaneous hydrolysis of the metal salt] were added dropwise an aminopolyalcohol [triethanolamine (1.00 mmol, 130 μL) for **1** or *N*-methyldiethanolamine (1.00 mmol, 116 μL) for **2**], an aqueous 1 M solution of sodium hydroxide (2.0 mL, 2.0 mmol) and potassium ferricyanide $K_3[Fe(CN)_6]$ (56 mg, 0.17 mmol) as a solid, in this order and with continuous stirring at room temperature. The obtained green solution was stirred overnight and left to evaporate in an open vial at ambient temperature (ca. 21 °C), resulting in the gradual formation, within several days, of a precipitate that was left unfiltered

(6) For selected examples of heterodimetallic frameworks based on the $[Fe(CN)_6]^{3-/4-}$ linkers, see: (a) Maji, T. K.; Pal, S.; Gurunatha, K. L.; Govindaraj, A.; Rao, C. N. R. *Dalton Trans.* **2009**, 4426. (b) Yanai, N.; Kaneko, W.; Yoneda, K.; Ohba, M.; Kitagawa, S. *J. Am. Chem. Soc.* **2007**, *129*, 3496. (c) Zhang, J.; Lachgar, A. *J. Am. Chem. Soc.* **2007**, *129*, 250. (d) Zhao, H.; Lopez, N.; Prosvirin, A.; Chifotides, H. T.; Dunbar, K. R. *Dalton Trans.* **2007**, 878. (e) Zhang, Y.-Z.; Duan, G.-P.; Sato, O.; Gao, S. *J. Mater. Chem.* **2006**, *16*, 2625. (f) Bonadio, F.; Senna, M.-C.; Ensling, J.; Sieber, A.; Neels, A.; Stoeckli-Evans, H.; Decurtins, S. *Inorg. Chem.* **2005**, *44*, 969. (g) Saha, M. K.; Moron, M. C.; Palacio, F.; Bernal, I. *Inorg. Chem.* **2005**, *44*, 1354. (h) Colacio, E.; Dominguez-Vera, J. M.; Lloret, F.; Rodriguez, A.; Stoeckli-Evans, H. *Inorg. Chem.* **2003**, *42*, 6962. (i) Figuerola, A.; Diaz, C.; Ribas, J.; Tangoulis, V.; Sangregorio, C.; Gatteschi, D.; Maestro, M.; Mahia, J. *Inorg. Chem.* **2003**, *42*, 5274.

(7) (a) Karabach, Y. Y.; Kirillov, A. M.; Haukka, M.; Sanchiz, J.; Kopylovich, M. N.; Pombeiro, A. J. L. *Cryst. Growth Des.* **2008**, *8*, 4100. (b) Kirillova, M. V.; Kirillov, A. M.; Guedes da Silva, M. F. C.; Pombeiro, A. J. L. *Eur. J. Inorg. Chem.* **2008**, 3423. (c) Jaremko, Ł.; Kirillov, A. M.; Smoleński, P.; Pombeiro, A. J. L. *Cryst. Growth Des.* **2009**, *9*, 3006. (d) Kirillov, A. M.; Smoleński, P.; Haukka, M.; Guedes da Silva, M. F. C.; Pombeiro, A. J. L. *Organometallics* **2009**, *28*, 1683.

(8) (a) Kirillov, A. M.; Kopylovich, M. N.; Kirillova, M. V.; Haukka, M.; Guedes da Silva, M. F. C.; Pombeiro, A. J. L. *Angew. Chem., Int. Ed.* **2005**, *44*, 4345. (b) Kirillova, M. V.; Kirillov, A. M.; Guedes da Silva, M. F. C.; Kopylovich, M. N.; Fraústo da Silva, J. J. R.; Pombeiro, A. J. L. *Inorg. Chim. Acta* **2008**, *361*, 1728. (c) Kirillova, M. V.; Guedes da Silva, M. F. C.; Kirillov, A. M.; Fraústo da Silva, J. J. R.; Pombeiro, A. J. L. *Inorg. Chim. Acta* **2007**, *360*, 506.

(9) (a) Karabach, Y. Y.; Kirillov, A. M.; Guedes da Silva, M. F. C.; Kopylovich, M. N.; Pombeiro, A. J. L. *Cryst. Growth Des.* **2006**, *6*, 2200. (b) Kirillov, A. M.; Karabach, Y. Y.; Haukka, M.; Guedes da Silva, M. F. C.; Sanchiz, J.; Kopylovich, M. N.; Pombeiro, A. J. L. *Inorg. Chem.* **2008**, *47*, 162. (c) Karabach, Y. Y.; Kirillov, A. M.; Haukka, M.; Kopylovich, M. N.; Pombeiro, A. J. L. *J. Inorg. Biochem.* **2008**, *102*, 1190. (d) Gruenwald, K. R.; Kirillov, A. M.; Haukka, M.; Sanchiz, J.; Pombeiro, A. J. L. *Dalton Trans.* **2009**, 2109. (e) Figiel, P. J.; Kirillov, A. M.; Karabach, Y. Y.; Kopylovich, M. N.; Pombeiro, A. J. L. *J. Mol. Catal. A: Chem.* **2009**, *305*, 178. (f) Kirillov, A. M.; Coelho, J. A. S.; Kirillova, M. V.; Guedes da Silva, M. F. C.; Nesterov, D. S.; Gruenwald, K. R.; Haukka, M.; Pombeiro, A. J. L. *Inorg. Chem.* **2010**, *49*, 6390.

(10) For selected examples of Cu/Fe coordination polymers bearing the $[Fe(CN)_6]^{3-/4-}$ linkers, see: (a) Rodriquez-Dieguez, A.; Kivekas, R.; Sillanpaa, R.; Cano, J.; Lloret, F.; Mckee, V.; Stoeckli-Evans, H.; Colacio, E. *Inorg. Chem.* **2006**, *45*, 10537. (b) Belicchi-Ferrari, M.; Bisceglie, F.; Casoli, C.; Durot, S.; Morgenstern-Badarau, I.; Pelosi, G.; Pilotti, E.; Pinelli, S.; Tarasconi, P. *J. Med. Chem.* **2005**, *48*, 1671. (c) Saha, M. K.; Lloret, F.; Bernal, I. *Inorg. Chem.* **2004**, *43*, 1969. (d) Coronado, E.; Gimenez-Saiz, C.; Nuez, A.; Sanchez, V.; Romero, F. M. *Eur. J. Inorg. Chem.* **2003**, 4289. (e) Mondal, N.; Saha, M. K.; Bag, B.; Mitra, S.; Gramlich, V.; Ribas, J.; Salah El Fallah, M. *J. Chem. Soc., Dalton Trans.* **2000**, 1601. (f) Colacio, E.; Dominguez-Vera, J.-M.; Ghazi, M.; Kivekas, R.; Moreno, J. M.; Pajunen, A. *J. Chem. Soc., Dalton Trans.* **2000**, 505.

(11) Farrusseng, D.; Aguado, S.; Pinel, C. *Angew. Chem., Int. Ed.* **2009**, *48*, 7502.

Table 1. Crystal Data and Structure Refinement Details for Compounds **1** and **2**

	1	**2**
empirical formula	$C_{42}H_{84}Cu_6FeN_{12}O_{18}$	$C_{36}H_{72}Cu_6FeN_{13}O_{15}$
Fw	1482.30	1364.16
T (K)	150(2)	150(2)
λ (Å)	0.71073	0.71073
crystal system	trigonal	triclinic
space group	$R\bar{3}:h$	$P\bar{1}$
a (Å)	18.542(3)	14.3634(13)
b (Å)	18.542(3)	15.9165(15)
c (Å)	19.724(4)	17.4598(16)
α (deg)		68.162(4)
β (deg)		66.272(5)
γ (deg)		64.600(3)
V (Å^3)	5872.7(14)	3203.6(5)
Z	3	2
ρ_{calcd} (g/cm^3)	1.257	1.414
μ(Mo Kα) (mm^{-1})	1.835	2.233
no. of collected reflns	48172	31219
no. of unique reflns	2388	14124
R_{int}	0.0440	0.0693
final $R1^a$, $wR2^b$ ($I \geq 2\sigma$)	0.0396, 0.0965	0.0556, 0.1225
GOF on F^2	1.156	0.921

^{a} $R1 = \sum||F_o| - |F_c||/\sum|F_o|$. ^{b} $wR2 = [\sum w(F_o^2 - F_c^2)^2/\sum w(F_o^2)^2]^{1/2}$.

(the main products do not crystallize if this intermediate solid is earlier removed by filtration). This precipitate then gradually disappears during the slow evaporation, within 2 weeks in air at ambient temperature, of the reaction mixture, giving rise to dark green cubic-shaped crystals (including those of X-ray quality) of the final products, which were collected and dried in air to furnish compounds **1** and **2** in about 40% yields based on copper(II) nitrate. The yields can be further increased up to about 60% if the last step of the crystallization (i.e., after the appearance of the first crop of crystals) is performed at a low temperature (ca. 5 °C).

$[Cu_6(H_2tea)_6Fe(CN)_6]_n(NO_3)_{2n}\cdot 6nH_2O$ (1). Found: C, 29.19; H, 5.78; N, 11.16. $C_{42}H_{96}Cu_6FeN_{14}O_{30}$ (1714.4) requires C, 29.42; H, 5.64; N, 11.44. FT-IR (KBr): 3402 (s br.) and 3251 (m br.) $\nu(H_2O)+\nu(OH)$, 2976 (w), 2921 (w), 2891 (w) and 2858 (w) $\nu(CH)$, 2093 (vs) $\nu(CN)$, 1653 (m br.) $\delta(H_2O)$, 1384 (vs) $\nu(NO_3)$, 1081 (s), 1040 (w), 903 (m), 637 (w), 587 (w) and 509 (m) cm^{-1}.

$[Cu_6(Hmdea)_6Fe(CN)_6]_n(NO_3)_{2n}\cdot 7nH_2O$ (2). Found: C, 27.72; H, 5.42; N, 12.58. $C_{36}H_{86}Cu_6FeN_{14}O_{25}$ (1552.3) requires C, 27.86; H, 5.58; N, 12.63. FT-IR (KBr): 3447 (s br.) and 3260 (m br.) $\nu(H_2O)+\nu(OH)$, 2975 (w), 2915 (w) and 2869 (w) $\nu(CH)$, 2095 (s) $\nu(CN)$, 1629 (w br.) $\delta(H_2O)$, 1384 (s) $\nu(NO_3)$, 1065 (m), 1023 (w), 995 (w), 895 (w), 633 (w), 592 (w) and 507 (w) cm^{-1}.

X-ray Crystal Structure Determinations. The X-ray diffraction data of **1** and **2** were collected using a Bruker AXS-KAPPA APEX II diffractometer with graphite monochromated Mo−Kα radiation. Data were collected using ω scans of 0.5° per frame, and a full sphere of data was obtained. Cell parameters were retrieved using Bruker SMART software and refined using Bruker SAINT on all the observed reflections. Absorption corrections were applied using SADABS.[12] Structures were solved by direct methods using the SHELXS−97 package and refined with SHELXL−97.[13a] Calculations were performed with the WinGX System-Version 1.80.03.[13b] All hydrogens were inserted in calculated positions. Heavily disordered nitrate anions and crystallization water molecules (some of them were partially lost) in the large accessible voids of **1** and **2** could not be modeled satisfactorily and thus were handled with PLATON/SQUEEZE.[14] Crystal data and details of data collection for **1** and **2** are reported in Table 1.

(12) *APEX2 & SAINT*; AXS Inc.: Madison, WI, 2004.
(13) (a) Sheldrick, G. M. *Acta Crystallogr.* **2008**, *A64*, 112. (b) Farrugia, L. J. *J. Appl. Crystallogr.* **1999**, *32*, 837.
(14) Spek, A. L. *Acta Crystallogr.* **1990**, *C46*, C34.

Scheme 1. Aqueous-Medium Self-Assembly Synthesis of Heterometallic Cu^{II}/Fe^{II} Metal-Organic Frameworks

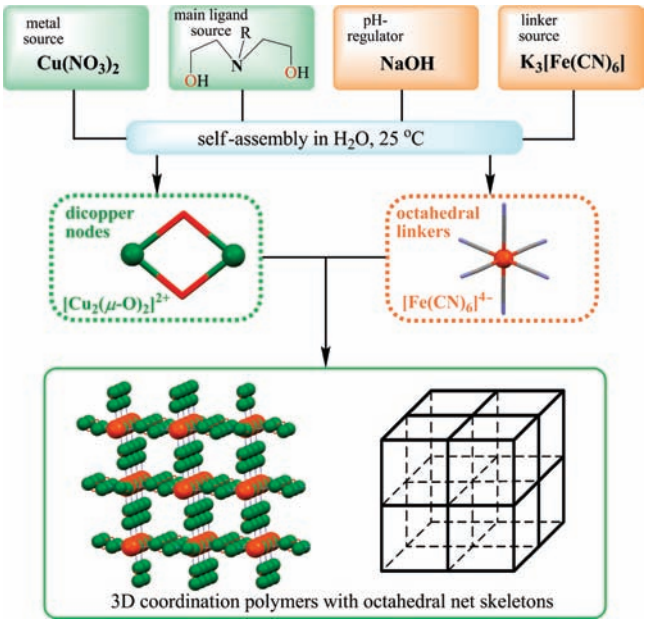

Catalytic Activity Studies in the Peroxidative Oxidation of Cyclohexane. In a typical experiment, the reaction mixture was prepared as follows: to 1.0 μmol of catalyst precursor **1** or **2** contained in the reaction flask were added 4.0 mL of MeCN solvent, 0−50 μmol (typically 30 μmol) of an acid promoter (aq. 7.0% HNO_3 or aq. 3.7% HCl), 1.0−5.0 mmol of C_6H_{12} substrate, and an excess (5.0−30.0 mmol) of H_2O_2 oxidant (30% in H_2O), in this order. The reaction mixture was stirred for 6 h at 25 °C in air (1 atm); then 90 μL of cycloheptanone (as internal standard), diethyl ether (typically 9.5 mL to extract the substrate and the products from the reaction mixture) were added. The resulting mixture was stirred for 15 min, and then a sample taken from the organic phase was analyzed by gas chromatography (GC) using a Fisons Instruments GC 8000 series gas chromatograph with a DB-WAX (J&W) capillary column and the Jasco-Borwin v.1.50 software.

In some cases, additional GC analyses were carried out after treatment with PPh_3 (for prior reduction of cyclohexyl hydroperoxide if formed),[15] which showed almost similar results to those analyses performed before the addition of PPh_3 in the systems promoted by HNO_3. However, a variation between the cyclohexanol and cyclohexanone ratio was observed in the systems promoted by HCl, thus indicating the presence of cyclohexyl hydroperoxide in the reaction mixtures even after a prolonged reaction time (24 h). Additional experiments were also undertaken in the presence of the radical traps $CBrCl_3$, 2,6-di-*tert*-butyl-4-methylphenol (BHT) or Ph_2NH (added before H_2O_2 in separate batches), resulting in a remarkable suppression of the catalytic activity.

The GC analyses of the aqueous phase revealed the presence of only traces (less than 0.1%) of oxidation products. Blank experiments were also performed with different amounts of H_2O_2 and other reagents, and confirmed that no cyclohexane oxidation products (or only traces, below 0.4%) were obtained in the absence of the metal catalyst precursor.

Results and Discussion

Synthesis and Spectroscopic Characterization. Recently, we have prepared via aqueous-medium self-assembly a

(15) (a) Shul'pin, G. B. *Mini-Rev. Org. Chem.* **2009**, *6*, 95. (b) Shul'pin, G. B. *J. Mol. Catal. A: Chem.* **2002**, *189*, 39. (c) Shul'pin, G. B. *C. R. Chim.* **2003**, *6*, 163.

Scheme 2. Structural Formulae (Repeating Units) of **1** and **2**[a]

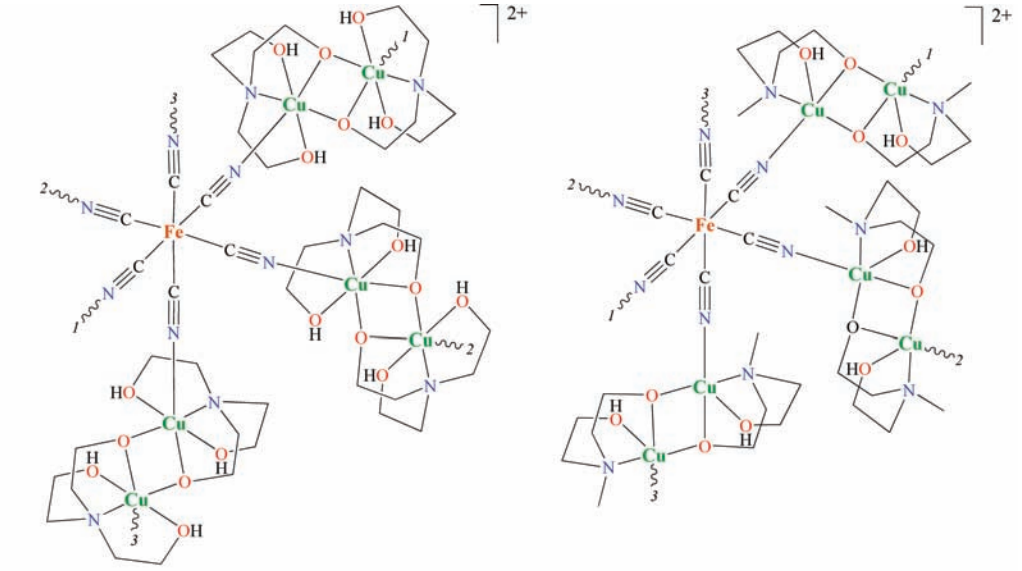

$[Cu_6(H_2tea)_6Fe(CN)_6]_n(NO_3)_{2n}\cdot 6nH_2O$ **(1)**

$[Cu_6(Hmdea)_6Fe(CN)_6]_n(NO_3)_{2n}\cdot 7nH_2O$ **(2)**

[a] Numbers indicate the extensions of polymeric chains.

series of Cu^{II} coordination polymers constructed from different Cu-aminopolyalcoholate building blocks (nodes) and various aromatic polycarboxylates (linkers).[9] Being interested in extending the type of such metal−organic materials to heterometallic coordination polymers, we have attempted a similar synthetic strategy by employing an iron-containing linker (hexacyannoferrate) instead of aromatic polycarboxylates. Thus, the combination in aqueous solution, in air and at 25 °C, of copper(II) nitrate as a metal source with either triethanolamine (H_3tea) or *N*-methyldiethanolamine (H_2mdea) as a main ligand source, followed by the alkalization of the obtained reaction mixture with sodium hydroxide (pH-regulator) and the addition of potassium ferricyanide $K_3[Fe(CN)_6]$ as a linker source (Scheme 1), results in the self-assembly generation of the new 3D heterometallic Cu^{II}/Fe^{II} coordination polymers $[Cu_6(H_2tea)_6Fe(CN)_6]_n(NO_3)_{2n}\cdot 6nH_2O$ (**1**) and $[Cu_6(Hmdea)_6Fe(CN)_6]_n(NO_3)_{2n}\cdot 7nH_2O$ (**2**) (Scheme 2). Although one would expect the formation of a Cu^{II}/Fe^{III} compound, the resulting coordination polymers **1** and **2** bear the reduced hexacyanoferrate(II) linkers, as clearly confirmed by IR spectroscopy and magnetic susceptibility measurements (see below). In fact, the spontaneous reduction of the ferricyanide $[Fe(CN)_6]^{3-}$ to ferrocyanide $[Fe(CN)_6]^{4-}$ anions in water and in the presence of Cu^{II} species has been already reported in a number of cases.[16] However, the mechanism of such a reduction still remains unclear. The syntheses of **1** and **2** are well reproducible, and both compounds have been isolated as dark green air-stable crystalline solids in about 40−60% yields (based on Cu^{II} nitrate). They have been characterized by IR spectroscopy, elemental and differential thermal analyses, magnetic susceptibility measurements, and single-crystal X-ray diffraction analyses.

In the course of the self-assembly syntheses of **1** and **2** the pH values varied from about 1.0 to 1.1 upon addition of H_3tea or H_2mdea to an acidic copper(II) nitrate solution, and then to about 8.5−9.5 after introducing NaOH and $K_3[Fe(CN)_6]$. The use of alkali medium is essential since **1** and **2** cannot be generated in the absence of NaOH or at low pH values (< 6.0) because of the formation and precipitation of an insoluble amorphous aminopolyalcoholato Cu species. In the absence of $K_3[Fe(CN)_6]$, the formation of soluble $[Cu_2(\mu\text{-}H_2tea)_2]^{2+}$ or $[Cu_2(\mu\text{-}Hmdea)_2]^{2+}$ species is observed which, however, cannot be crystallized unless an auxiliary ligand (e.g., benzenecarboxylate, azide, or thiocyanate) or a linker (e.g., benzenepolycarboxylate or cyanometallate) is added.[9b,d,18c]

The IR spectra of **1** and **2** are rather similar, showing typical vibrations for the Cu-aminopolyalcoholate and hexacyanoferrate(II) moieties, as well as for nitrate ions and crystallization water molecules.[17] Hence, the characteristic bands in the 3450−3250 cm^{-1} range are assigned to ν(OH) and $\nu(H_2O)$ vibrations, their broad character being associated with multiple hydrogen bonding interactions. In addition, the less intense bands at 1653 (**1**) or 1629 (**2**) cm^{-1} correspond to $\delta(H_2O)$ vibrations. Several bands due to ν_{as} and ν_s(CH) vibrations are also observed in the 2980−2855 cm^{-1} range. The detection of strong ν(CN) adsorptions with maxima at 2093 (**1**) or 2095 (**2**) cm^{-1} clearly supports the presence of the $[Fe(CN)_6]^{4-}$ moieties, which are typically observed in the 2110−2050 cm^{-1} range,[16a,17] while the corresponding

(16) (a) Triki, S.; Sala-Pala, J.; Thétiot, F.; Gómez-García, C. J.; Daran, J.-C. *Eur. J. Inorg. Chem.* **2006**, 185. (b) Shen, X.-P.; Li, Y.-Z.; Yuan, A.-H.; Xu, Z. *J. Mol. Struct.* **2005**, *754*, 106. (c) Thetiot, F.; Triki, S.; Sala Pala, J. *New J. Chem.* **2002**, *26*, 196. (d) Parker, R. J.; Spiccia, L.; Batten, S. R.; Cashion, J. D.; Fallon, G. D. *Inorg. Chem.* **2001**, *40*, 4696. (e) Sun, X.; Wang, Z.; Chen, Z.; Bian, J.; Yan, C.; Xu, G. *Prog. Nat. Sci.* **1999**, *9*, 425.

(17) Nakamoto, K. *Infrared and Raman Spectra of Inorganic and Coordination Compounds*, 5th ed; Wiley: New York, 1997.

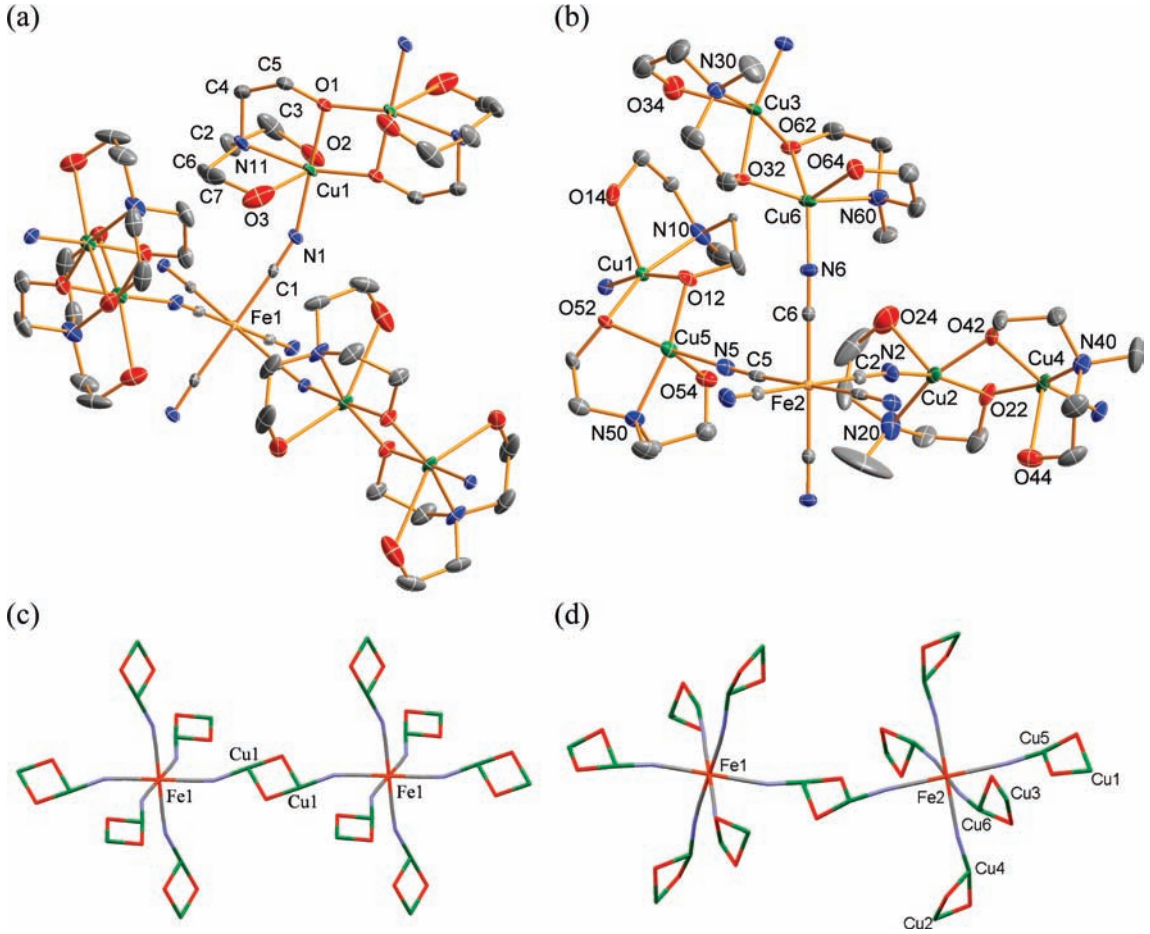

Figure 1. Structural fragments of **1** (a, c) and **2** (b, d) with the partial atom labeling scheme; (a, b): displacement ellipsoid (50% probability) plots (H atoms are omitted for clarity); (c, d): capped stick plots showing the relative spatial orientation of the $[Cu_2(\mu\text{-}O)_2]^{2+}$ nodes and the $[Fe(CN)_6]^{4-}$ linkers (H_2tea and Hmdea moieties, except for μ-O atoms, are omitted for clarity). Fe orange, Cu green, N blue, O red, C gray.

Fe^{III} species, $[Fe(CN)_6]^{3-}$, should absorb at higher wavenumbers (2180−2150 cm^{-1}). The spectra of both compounds also feature strong bands with maxima at 1384 cm^{-1} due to $\nu(NO_3)$ vibrations. In addition, there are a number of bands (1100−900 cm^{-1}) in the spectra of **1** and **2** that are associated to ν(C-X) (X = C, N, O) vibrations of H_2tea or Hmdea ligands.

X-ray Crystal Structures. The single-crystal X-ray analyses of **1** and **2** show that both compounds are constructed from $[Cu_2(\mu\text{-aminopolyalcoholate})_2]^{2+}$ nodes and octahedral hexacyanoferrate(II) linkers, resulting in the formation of 3D metal−organic frameworks. Although the $[Fe(CN)_6]^{3-/4-}$ species have been broadly used in the design of coordination polymers,[5,6,10] one should mention that a search of the literature and the Cambridge Structural Database (CSD)[3] revealed only three examples[16a,b,e] of such 3D heterometallic Cu/Fe metal−organic frameworks which, moreover, are rather distinct from those of **1** and **2**.

The structural fragments of **1** and **2** showing the ellipsoid plots and the relative spatial orientation of the $[Cu_2(\mu\text{-}O)_2]^{2+}$ and $[Fe(CN)_6]^{4-}$ units with the generation of cross-linking motifs are depicted in Figure 1. The selected bonding parameters and the shortest metal−metal separations are collected in Tables 2 and 3, respectively. Additional crystal packing diagrams of **1** and **2** are represented in Figure 2, and Supporting Information, Figures S1 and S2. The symmetry codes along the discussion below are those of Table 2.

$[Cu_6(H_2tea)_6Fe(CN)_6]_n(NO_3)_{2n}\cdot 6nH_2O$ (1). The crystal structure of **1** bears the three symmetry equivalent dicopper(II) $[Cu_2(H_2tea)_2]^{2+}$ units per one hexacyanoferrate(II) μ_6-$[Fe(CN)_6]^{4-}$ moiety (Figure 1a). Inversion centers are positioned in the $[Cu_2(H_2tea)_2]^{2+}$ nodes which are constructed from two H_2tea ligands and two equivalent Cu1 atoms, the latter featuring a heavily distorted octahedral geometry. The tetradentate *N*,O_3-triethanolaminate ligands are monodeprotonated at the bridging oxygen atoms (O1) which occupy, along with the amino (N11) and the cyano (N1) nitrogen atoms, the basal positions. The two remaining H_2tea oxygen atoms (O2, O3) lie in apical sites, being bent [O2−Cu1−O3 148.17(11)°] outward from the center of the $[Cu_2(\mu\text{-}O)_2]^{2+}$ core. These apical O atoms are bound through the Cu1−O2 [2.409(3) Å] and Cu1−O3 [2.717(4) Å] bonds, which are significantly elongated in comparison to the basal Cu1−O1 [avg. 1.932(3) Å] distances. The binding of the H_2tea involves three five-membered Cu−N−C−C−O chelate rings with the bite O−Cu1−N11 angles ranging from 73.27(12) [O3−Cu1−N11] to 83.55(13)° [O1−Cu1−N11]. The $[Cu_2(\mu\text{-}O)_2]^{2+}$ core is planar (Figure 1a) and has the Cu1···$Cu1^i$ separation of 2.9855(8) Å, while the representative Cu1−O1−$Cu1^i$ and O1−Cu1−$O1^i$ angles are 101.32(14) and 78.68(12)°, respectively. In general, the bonding parameters within the $[Cu_2(H_2tea)_2]^{2+}$ nodes in **1** (Table 2) are

Table 2. Selected Bond Lengths (Å) and Angles (deg) for **1** and **2**[a]

Compound **1**			
Cu1−O1	1.935(3)	O2−Cu1−O3	148.17(11)
Cu1−O1^{i}	1.926(3)	O1^{i}−Cu1-N11	83.55(13)
Cu1−O2	2.409(3)	O2−Cu1−N11	80.69(13)
Cu1−O3	2.717(4)	O3−Cu1−N11	73.27(12)
Cu1−N1	1.950(3)	Cu1−O1−Cu1^{i}	101.33(11)
Cu1−N11	2.073(4)	O1−Cu1−O1^{i}	78.68(11)
Fe1−C1	1.913(3)	Cu1−N1−C1	159.6(3)
Cu1···Cu1^{i}	2.9855(8)	Fe1−C1−N1	177.2(3)
O1−Cu1−N1	100.28(13)	C1−Fe1−C1^{ii}	90.50(16)
Compound **2**[b]			
Cu1−O12	1.955(4)	Fe2−C2	1.900(6)
Cu1−O52	1.973(3)	Cu1···Cu5	2.7793(9)
Cu1−O14	2.244(5)	O14−Cu1−N10	79.9(2)
Cu1−N1	1.932(5)	O12−Cu1−N10	84.74(17)
Cu1−N10	2.044(5)	O12−Cu1−O52	78.33(15)
Cu5−O12	1.960(5)	O12−Cu1−O14	100.05(17)
Cu5−O52	1.937(4)	Cu1−O12−Cu5	90.45(14)
Cu5−O54	2.361(5)	Cu1−O52−Cu5	90.63(14)
Cu5−N5	1.900(5)	Cu1−N1−C1	168.6(4)
Cu5−N50	2.043(6)	Fe2−C5−N5	175.5(5)
Fe2−C5	1.895(6)	C5−Fe2−C5^{i}	180.00

[a] Symmetry transformations used to generate equivalent atoms: **1**: (i) $1-x, -y, 1-z$; (ii) $1-y, x-y, z$; **2**: (i) $2-x, 1-y, -z$. [b] Bond distances and angles around the other two dicopper units (Cu2/Cu4 and Cu3/Cu6) and the other $[Fe(CN)_6]^{4-}$ moiety (Fe1) found in the unit cell of **2** are similar to those of the Cu1/Cu5 and Fe2 fragments presented here.

Table 3. Selected Shortest Metal−Metal Separations (Å) for **1** and **2**

	1	**2**
Cu···Cu (within node)	2.9855(8)	2.7793(9)
Cu···Fe (node-linker)	4.9276(11)	4.8819(9)
Cu···Cu (node-linker-node if bent)	6.929(1)	6.543(1)
Cu···Cu (node-linker-node if linear)	9.855(1)	9.876(1)
Fe···Fe (linker-node-linker)	12.563(2)	11.748(1)

comparable to those encountered in other compounds possessing the $[Cu_2(\mu\text{-aminopolyalcoholate})_2]^{2+}$ units.[8a,9b,9d,18]

In **1**, the $[Fe(CN)_6]^{4-}$ linkers exhibit an almost ideal octahedral geometry around the Fe1 atoms, which is composed of six symmetry equivalent cyano groups [avg. Fe−C 1.913(5) Å] (Table 2). Each of the cyano moieties acts as a bidentate bridging ligand, thus providing a simultaneous interconnection of the octahedral μ_6-$[Fe(CN)_6]^{4-}$ linkers with the six $[Cu_2(H_2tea)_2]^{2+}$ nodes (Figure 1c) to form a 3D metal−organic framework (Figure 2a), wherein the shortest node-linker Cu···Fe distance is 4.9276(11) Å. The Fe1−C1−N1 angle of 177.2(4)° is close to linear, while the corresponding Cu1−N1−C1 angle of 159.5(3)° is significantly bent. However, because of the symmetry of the $[Cu_2(\mu\text{-O})_2]^{2+}$ cores, the overall ~Fe-CN-$Cu_2(\mu$-O$)_2$-NC-Fe-CN-$Cu_2(\mu$-O$)_2$~ cross-linking motifs are almost linear, thus resulting in a regular octahedral net structure

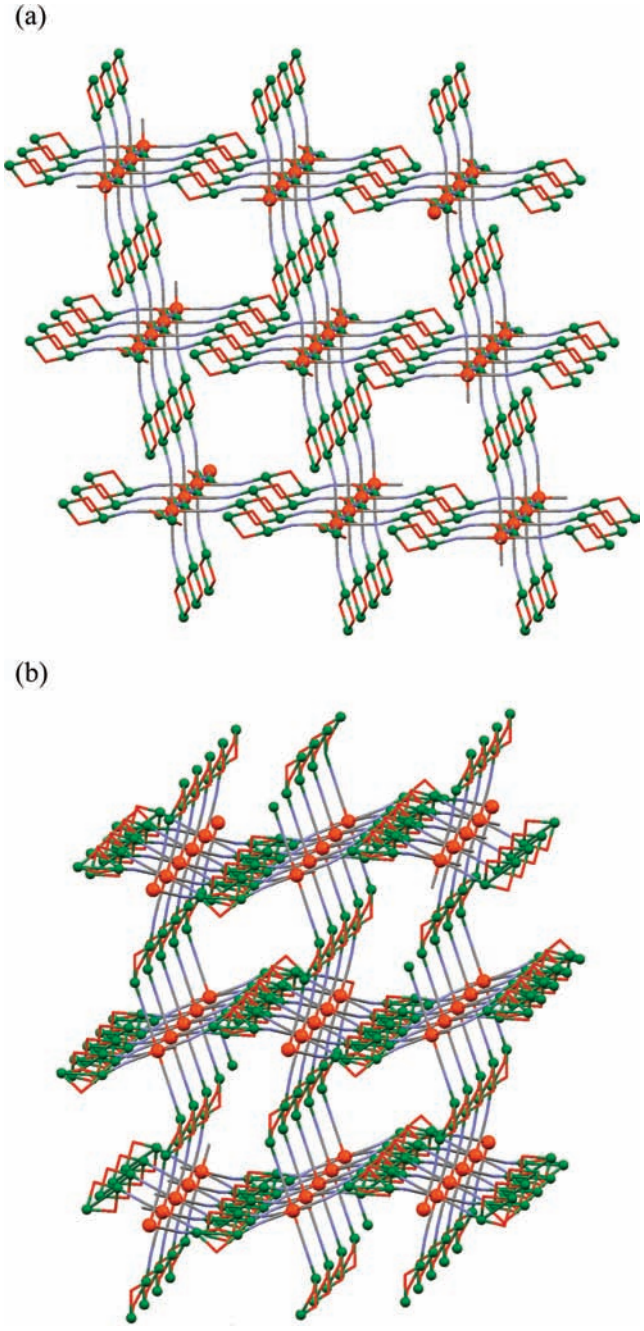

Figure 2. Simplified crystal packing diagrams of **1** (a) and **2** (b) showing their 3D metal−organic skeletons in a form of regular (**1**) and distorted (**2**) octahedral nets. H_2tea and Hmdea moieties (except for μ-O atoms) are omitted for clarity. Fe orange balls, Cu green balls, O red, N blue, and C gray.

(Figure 2a). In each particular motif, the $[Cu_2(H_2tea)_2]^{2+}$ units occupy identical spatial positions (Figure 1c), with angles of 53.21° between the non-coplanar planes formed by the $[Cu_2(\mu\text{-O})_2]^{2+}$ cores. Within those motifs, the shortest Cu···Cu (node-linker-node if linear) and Fe···Fe (linker-node-linker) separations are 9.855(1) and 12.563(2) Å, respectively, the former value being equivalent to half of the *c* unit cell dimension (Table 3). Besides, because of the high overall symmetry of the structure and the coplanarity of the $[Fe(CN)_6]^{4-}$ linkers, the 3D metal−organic framework in **1** features the presence of channels with the biggest diameter of

(18) (a) Kirillov, A. M.; Kopylovich, M. N.; Kirillova, M. V.; Karabach, E. Y.; Haukka, M.; Guedes da Silva, M. F. C.; Pombeiro, A. J. L. *Adv. Synth. Catal.* **2006**, *348*, 159. (b) Kirillov, A. M.; Haukka, M.; Kopylovich, M. N.; Pombeiro, A. J. L. *Acta Crystallogr.* **2007**, *E63*, m526. (c) Figiel, P. J.; Kirillov, A. M.; Guedes da Silva, M. F. C.; Lasri, J.; Pombeiro, A. J. L. *Dalton Trans.* **2010**, *39*, 9879. (d) Marin, G.; Tudor, V.; Kravtsov, V. C.; Schmidtmann, M.; Simonov, Y. A.; Müller, A.; Andruh, M. *Cryst. Growth Des.* **2005**, *5*, 279. (e) Tudor, V.; Marin, G.; Kravtsov, V.; Simonov, Y. A.; Lipkowski, J.; Brezeanu, M.; Andruh, M. *Inorg. Chim. Acta* **2003**, *353*, 35. (f) Paraschiv, C.; Andruh, M.; Ferlay, S.; Hosseini, M. W.; Kyritsakas, N.; Planeix, J.-M.; Stanica, N. *Dalton Trans.* **2005**, 1195.

about 7.2 Å. These channels should host the nitrate ions and crystallization water molecules.

$[Cu_6(Hmdea)_6Fe(CN)_6]_n(NO_3)_{2n}\cdot 7nH_2O$ (2). In spite of some similarities between the crystal structures of **1** and **2**, the latter shows a number of distinctive features. Although the structure of **2** (Figure 1b) is composed of dicopper(II) nodes, $[Cu_2(Hmdea)_2]^{2+}$, that are related to those of **1**, and also of hexacyanoferrate(II) μ_6-$[Fe(CN)_6]^{4-}$ linkers, the main differences arise from its lower overall symmetry (i.e., the presence of six Cu and two Fe symmetry non-equivalent atoms) and nonplanarity of the $[Cu_2(\mu\text{-}O)_2]^{2+}$ cores. The latter possess pentacoordinated Cu atoms that adopt distorted square-pyramidal coordination environments (Figure 1b). The equatorial sites are filled by the two μ-O and amino N atoms from the tridentate Hmdea ligands, as well as by cyano N atoms from the $[Fe(CN)_6]^{4-}$ moieties. The remaining oxygen atoms of the Hmdea fragments are located in apical sites, being also spatially oriented into different directions. The main bonding parameters within the dicopper(II) nodes in **2** (Table 2) are comparable to those found in **1**, except the apical Cu1−O14 [2.243(5) Å] and Cu5−O54 [2.360(4) Å] bonds that are significantly shorter than those in **1** [i.e., 2.409(3) and 2.717(4) Å]. One should also mention that the nonplanar $[Cu_2(\mu\text{-}O)_2]^{2+}$ cores in **2** possess closer Cu···Cu separations [i.e., 2.7793(9) vs 2.9855(8) Å for **2** and **1**, respectively] because of their twisted-square geometries.

As in **1**, both the Fe1 and Fe2 hexacyanoferrate(II) linkers in **2** adopt almost ideal octahedral geometries, exhibiting Fe−C [avg. 1.904(6) Å] and Fe−C−N [avg. 176.7(6)°] bonding parameters (Table 2) that are comparable to those of **1** and of other Fe^{II}/Cu^{II} compounds comprising the $[Fe(CN)_6]^{4-}$ moieties.[16] The connection of the dicopper nodes with the $[Fe(CN)_6]^{4-}$ linkers [shortest Cu···Fe separation = 4.8819(9) Å] is realized through the less bent Cu−N−C angles [avg. 169.7(6)° in **2** vs 159.6(3)° in **1**] which, however, are different in each of the three symmetry non-equivalent nodes, ranging from 159.1(5) [Cu6−N6−C6] to 175.1(5)° [Cu3−N3−C3]. In addition, the angles between the planes defined by the $[Cu_2(\mu\text{-}O)_2]^{2+}$ cores are of 66.94 (Cu1Cu5/Cu3Cu6), 85.52 (Cu2Cu4/Cu3Cu6), and 86.60° (Cu2Cu4/Cu3Cu6). These differences, along with a low overall symmetry of **2**, contribute to a distinct spatial orientation pattern of nodes and linkers (Figure 1d). As a result, the overall ∼Fe-CN-$Cu_2(\mu\text{-}O)_2$-NC-Fe-CN-$Cu_2(\mu\text{-}O)_2$∼ cross-linking motifs have a wave-like shape, thus bringing a distortion to an octahedral 3D net structure of **2** (Figure 2b). As a consequence, the shortest Cu···Cu (node-linker-node if bent) and Fe ···Fe (linker-node-linker) separations of 6.543(1) and 11.748(1) Å, respectively, are about 0.4 or 0.8 Å inferior to the corresponding distances in **1** (Table 3). The structure of **2** features also the presence of guest nitrate ions and crystallization water molecules within the channels of the 3D net which, however, possess smaller size (ca. 4.4 Å diameter) because of an overall distortion of the metal−organic framework.

Magnetic Properties. The temperature dependence of the $\chi_M T$ product for compound **1** is shown in Figure 3a (χ_M is the molar magnetic susceptibility which considers six copper(II) ions). The value observed for $\chi_M T$ at room temperature, $\chi_M T = 1.80\ cm^3\ mol^{-1}\ K$, is lower than the expected one for six non-interacting copper(II) ions [$\chi_M T = 6 \times (N\beta^2 g^2_{Cu}/3kT) S_{Cu}(S_{Cu}+1) \approx 2.48\ cm^3\ mol^{-1}\ K$, wherein $g_{Cu} \approx 2.10$ stands for the Landé factor, β the Bohr magneton, k the Boltzman constant, and $S_{Cu} = 1/2$].[19] The $\chi_M T$ values continuously decrease upon cooling, reaching an almost zero value below 40 K. The $\chi_M T$ values and the shape of the plot denote a rather strong antiferromagnetic coupling. The structure of compound **1** consists of μ-O-alkoxo bridged dicopper(II) nodes linked by the diamagnetic $[Fe(CN)_6]^{4-}$ groups to yield a 3D network having three copper(II) dimers *per* molecular formula. Hexacyanoferrate(II) anions have been observed to mediate either weak ferro-,[16c] weak antiferromagnetic[16b] or even are said to be unable to mediate any kind of magnetic coupling, while the μ-O-alkoxo bridges are known to mediate efficiently the magnetic interaction.[9b,d,16d] Under this approach the interaction via the $[Fe(CN)_6]^{4-}$ moieties is discarded and the strong antiferromagnetic coupling is considered to take place through the μ-O-alkoxo bridges, the compound thus behaving as antiferromagnetically coupled dicopper(II) complexes. Hence, the magnetic

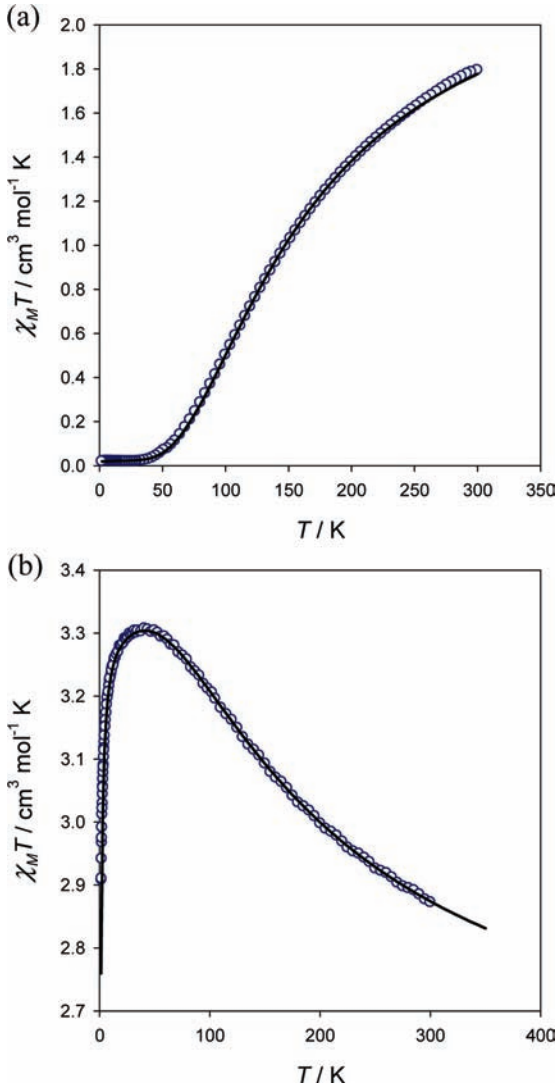

Figure 3. Temperature dependences of the $\chi_M T$ product for compounds **1** (a) and **2** (b). The solid lines correspond to best fits to copper(II) dinuclear models; see text for further details.

(19) Kahn, O. *Molecular Magnetism*; VCH: New York, 1993.

data have been analyzed by means of the Bleaney−Bowers expression for two interacting spin doublets, eq 1, which considers the isotropic spin Hamiltonian $H = -J(\boldsymbol{S}_1\boldsymbol{S}_2)$.[19]

$$\chi_M = 3 \times \frac{N\beta^2 g^2}{3kT}\left[\frac{6}{3+\exp(-J/kT)}\right] \qquad (1)$$

The factor 3 takes into account the three dicopper(II) nodes occurring in **1**, and J is the intra-dimer magnetic exchange coupling constant. Best fit parameters to eq 1 are $g = 2.07(1)$, $J = -199(1)\ cm^{-1}$, and $R = 4.87 \times 10^{-4}$. R is the agreement factor defined as $\sum_i[(\chi_M T)_{obs}(i) - (\chi_M T)_{calc}(i)]^2/\sum_i[(\chi_M T)_{obs}(i)]^2$. Paramagnetic impurities as mononuclear species are found to be $\rho = 0.01$. The magnetic data show a good agreement with the dinuclear model as can be seen in Figure 3a, and the interactions through the $[Fe(CN)_6]^{4-}$ groups are not further considered in **1**.

The temperature dependence of the $\chi_M T$ product for **2** is shown in Figure 3b (here, again, χ_M is the molar magnetic susceptibility which considers six copper(II) ions). At room temperature, $\chi_M T$ is 2.82 $cm^3\ mol^{-1}$ K, a value which is above the expected one for six uncoupled Cu(II) ions [$\chi_M T = 6 \times (N\beta^2 g^2_{Cu}/3kT)S_{Cu}(S_{Cu}+1) \approx 2.48\ cm^3\ mol^{-1}$ K; with $g_{Cu} = 2.10$ and $S_{Cu} = 1/2$]. The $\chi_M T$ value increases on cooling and reaches a maximum value of 3.26 $cm^3\ mol^{-1}$ K that corresponds to three copper(II) dinuclear complexes with a $S = 1$ total spin ground state. These features are indicative of an overall strong ferromagnetic coupling between the copper(II) ions in **2**. The decrease of $\chi_M T$ at low temperatures is ascribed to zero-field-splitting effects and/or weak intermolecular interactions through the diamagnetic $[Fe(CN)_6]^{4-}$ groups.

Under this approach the magnetic data of compound **2** have been fitted to the same model as compound **1** with the inclusion of a zero-field-splitting term and a Weiss parameter to consider the interactions through the $[Fe(CN)_6]^{4-}$ groups as intermolecular interactions.[19] Best fit parameters are $g = 2.10(1)$, $J = +153(1)\ cm^{-1}$, $D = -0.30\ cm^{-1}$, $\theta = -1.06$ K, and $R = 2.57 \times 10^{-4}$, the theoretical curve showing a good agreement with the magnetic data.

The nature and the strength of the magnetic exchange coupling in alkoxo and hydroxo bridged dinuclear copper(II) complexes are mainly affected by the Cu−O−Cu bond angles (Θ). In general, the antiferromagnetic couplings are observed for Θ > 98°, whereas the ferromagnetic couplings are observed for Θ < 98°.[20a] Other parameters, such as the trigonal distortion of the copper(II) environment, the out-of-plane shift of the carbon atom of the alkoxo bridge or the hinge distortion of the $[Cu_2(\mu\text{-}O)_2]^{2+}$ core, modulate the coupling[20b] and ferromagnetic couplings can be observed for slightly larger Θ angles.[9b] Both compounds compare well with other copper(II) complexes that show similar features,[9b,d] and confirm this correlation by displaying strong antiferromagnetic couplings for Θ = 101° and ferromagnetic couplings for a mean Θ = 90.5° in **1** and **2**, respectively.

Thermal Analysis. The differential thermal analysis of compounds **1** and **2** reveals seven thermal effects over the 30−750 °C temperature range (Supporting Information, Figure S3), and their summary is presented in Supporting Information, Table S1. For **1**, the endothermic process in the 30−120 °C range with maximum at 88 °C corresponds to the elimination of six water molecules of crystallization (the overall mass loss of 6.2% is in accord with the calculated value of 6.3%). A similar behavior is observed for **2**, wherein seven crystallization water molecules are released in the 30−130 °C range (maximum at 75 °C), corresponding to the mass loss of 8.4% (calculated 8.1%). The subsequent exothermic processes in the 110−177 (**1**) and 130−188 °C (**2**) temperature intervals are presumably associated with the decomposition of one or two nitrate anions, respectively. In **1**, the elimination of the second NO_3^- anion occurs during the next exothermic effect (177−230 °C), being overlapped with a multistep decomposition of organic moieties. The latter process takes place also in **2**, starting at 188 °C (Supporting Information, Table S1).

An interesting feature of compound **1** consists of the possibility to reversibly readsorb water. In fact, when a completely dehydrated sample (after heating up to 120 °C) was placed in water solution for 4 h, then dried in air and subjected to thermal analysis, all the curves were identical to those of the initial sample **1** (Supporting Information, Figure S3a), revealing the readsorption of 6 water molecules. Such a removal and inclusion of water can be repeated several times. Furthermore, the repetition of the above procedure using a methanol solution instead of water resulted in reversible binding and escape processes involving 2.5 methanol molecules. However, under similar conditions, the dehydrated sample of **2** is capable of adsorbing only about 3.5 water or one methanol molecule, presumably because of the higher distortion of its metal−organic framework. The attempts to use the dehydrated samples of **1** and **2** for an uptake of the less polar acetone were not successful, what is eventually associated either with the small size of channels in **1** and **2** or with the lack of strong H-bonding interactions between acetone molecules and the host metal−organic framework. Other metal−organic materials possessing some related features on the reversible water binding and escape processes were recently reported.[6a,21]

Mild Peroxidative Oxidation of Cyclohexane. In pursuit of our general interest in the development of new catalytic systems for the mild oxidative functionalization of alkanes through selective oxygenation[22] or

(20) (a) Crawford, V. H.; Richardson, H. W.; Wasson, J. R.; Hodgson, D. J.; Hatfield, W. E. *Inorg. Chem.* **1976**, *15*, 2107. (b) Ruiz, E.; Alemany, P.; Alvarez, S.; Cano, J. *J. Am. Chem. Soc.* **1997**, *119*, 1297.

(21) (a) Yanai, N.; Kaneko, W.; Yoneda, K.; Ohba, M.; Kitagawa, S. *J. Am. Chem. Soc.* **2007**, *129*, 3496. (b) Zhang, J.; Lachgar, A. *J. Am. Chem. Soc.* **2007**, *129*, 250. (c) Fernandes, R. R.; Kirillov, A. M.; Guedes da Silva, M. F. C.; Ma, Z.; da Silva, J. A. L.; Fraústo da Silva, J. J. R.; Pombeiro, A. J. L. *Cryst. Growth Des.* **2008**, *8*, 782. (d) Sereda, O.; Stoeckli, F.; Stoeckli-Evans, H.; Dolomanov, O.; Filinchuk, Y.; Pattison, P. *Cryst. Growth Des.* **2009**, *9*, 3104. (e) Sereda, O.; Stoeckli-Evans, H.; Dolomanov, O.; Filinchuk, Y.; Pattison, P. *Cryst. Growth Des.* **2009**, *9*, 3168. (f) Henninger, S. K.; Habib, H. A.; Janiak, C. *J. Am. Chem. Soc.* **2009**, *131*, 2776.

(22) (a) Kirillova, M. V.; Kozlov, Y. N.; Shul'pina, L. S.; Lyakin, O. Y.; Kirillov, A. M.; Talsi, E. P.; Pombeiro, A. J. L.; Shul'pin, G. B. *J. Catal.* **2009**, *268*, 26. (b) Kirillova, M. V.; Kirillov, A. M.; Mandelli, D.; Carvalho, W. A.; Pombeiro, A. J. L.; Shul'pin, G. B. *J. Catal.* **2010**, *272*, 9. (c) Di Nicola, C.; Karabach, Y. Y.; Kirillov, A. M.; Monari, M.; Pandolfo, L.; Pettinari, C.; Pombeiro, A. J. L. *Inorg. Chem.* **2007**, *46*, 221. (d) Nesterov, D. S.; Kokozay, V. N.; Dyakonenko, V. V.; Shishkin, O. V.; Jezierska, J.; Ozarowski, A.; Kirillov, A. M.; Kopylovich, M. N.; Pombeiro, A. J. L. *Chem. Commun.* **2006**, 4605. (e) Contaldi, S.; Di Nicola, C.; Garau, F.; Karabach, Y. Y.; Martins, L. M. D. R. S.; Monari, M.; Pandolfo, L.; Pettinari, C.; Pombeiro, A. J. L. *Dalton Trans.* **2009**, 4928. (f) Silva, T. F. S.; Mishra, G. S.; Guedes da Silva, M. F. C.; Wanke, R.; Martins, L. M. D. R. S.; Pombeiro, A. J. L. *Dalton Trans.* **2009**, 9207.

Table 4. Mild Oxidation of Cyclohexane by Hydrogen Peroxide in the Presence of **1** and **2**[a]

				yield of products, %[b]			
entry	catalyst precursor	acid promoter	n(acid)/n(cat. precursor)	cyclohexanol	cyclohexanone	total[c]	TON[d]
1	**1**	–	0	0.6	0.5	1.1	11
2	**1**	HNO_3	10	2.3	3.4	5.7	57
3	**1**	HNO_3	20	2.9	5.8	8.7	87
4	**1**	HNO_3	30	3.8	7.2	11.0	110
5	**1**	HNO_3	50	2.9	2.6	5.5	55
6	**2**	–	0	0.8	0.5	1.3	13
7	**2**	HNO_3	10	1.6	6.5	8.1	81
8	**2**	HNO_3	20	3.1	9.6	12.7	127
9	**2**	HNO_3	30	4.0	10.1	14.1	141
10	**2**	HNO_3	50	6.8	3.8	10.6	106
11[e]	**1**	HCl	30	10.4	1.5	11.9	119
12[e]	**2**	HCl	30	14.0	1.8	15.8	158
13[f,g]	**1**	HCl	30	15.6	1.2	16.8	168
14[f,g]	**2**	HCl	30	19.5	2.0	21.5	215
15[h]	**1**	HNO_3	30	1.9	4.5	6.4	319
16[h]	**2**	HNO_3	30	2.0	4.8	6.8	339
17[h,g]	**1**	HCl	30	4.7	1.6	6.3	315
18[h,g]	**2**	HCl	30	6.8	2.5	9.3	467

[a] Reaction conditions (unless stated otherwise): catalyst precursor (1.0 μmol), C_6H_{12} (1.0 mmol), MeCN (4.0 mL), acid promoter (0−50 μmol), H_2O_2 (30% in H_2O, 15.0 mmol), 6 h, 25 °C. [b] Moles of product/100 mols of cyclohexane. [c] Cyclohexanol + cyclohexanone. [d] Overall TON values (moles of products/mol of catalyst precursor). [e] H_2O_2 (30% in H_2O, 5.0 mmol). [f] H_2O_2 (30% in H_2O, 10.0 mmol). [g] GC analysis after treatment with PPh_3. [h] C_6H_{12} (5.0 mmol), H_2O_2 (30% in H_2O, 30.0 mmol), 24 h.

Scheme 3. Mild Peroxidative Oxidation of Cyclohexane to Cyclohexanol and Cyclohexanone

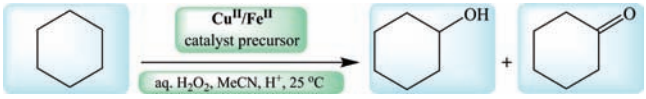

carboxylation[23] reactions, we have recently reported the application of various Cu-aminopolyalcoholate coordination polymers in such types of oxidative transformations.[8a,9c−9f,18a] Bearing in mind that compounds **1** and **2** are somehow related to those Cu catalytic systems and, in addition, possess extra iron(II) centers, we have evaluated their catalytic potential for the mild peroxidative oxidation of cyclohexane to cyclohexanol and cyclohexanone (Scheme 3). This transformation has been used as a recognized model reaction,[24a] also in view of the importance of the products, since cyclohexanol and cyclohexanone are intermediates in nylon-6,6′ and polyamide-6 productions.[24b,c] The catalytic tests were undertaken by reacting cyclohexane, at 25 °C in MeCN medium, with aqueous H_2O_2 in the presence of the catalyst precursor (compound **1** or **2**) and an acid promoter (HNO_3 or HCl). The obtained results are summarized in Table 4.

As expected, in the absence of an acid promoter, compounds **1** and **2** are not soluble in the reaction mixture (heterogeneous system) and are barely active, leading to only about 1% overall yields of products, based on cyclohexane (Table 4, entries 1, 6). This is presumably associated with a strong catalase activity, which is more pronounced when using higher amounts of a catalyst precursor (i.e., 10.0 vs 1.0 μmol). Such type of behavior was previously observed in some other systems composed of iron containing catalyst precursors.[22d,25] However, in the presence of an acid promoter, compounds **1** and **2** dissolve in the reaction mixture (homogeneous catalytic system), acting as active catalyst precursors for the oxidation of cyclohexane. Hence, the addition of 10 equiv (relative to the catalyst precursor) of nitric acid leads to a noticeable product yield growth up to 5.7 or 8.1%, when using compounds **1** or **2**, respectively (entries 2, 7). The total yields reach maximum values of 11.0 (for **1**) and 14.1% (for **2**) with cyclohexanone being the major product, at the HNO_3-to-catalyst precursor molar ratio of 30:1 (entries 4, 9), beyond which the yields respectively drop to 5.5 and 10.5% (entries 5, 10), in the presence of 50 equiv of HNO_3.

Following our recent study that disclosed an unusual promoting behavior of HCl in the Cu-catalyzed oxidation of cyclohexane,[22a] we have also tested this acid in the present systems. As a result, slightly higher total yields of 11.9 (for **1**) and 15.8% (for **2**) are obtained, using even a lower amount of oxidant (Table 4, entries 11, 12). However, these yields grow further upon increasing the oxidant-to-catalyst molar ratio from 5000:1 to 10000:1, reaching the values of 16.8 and 21.5% for **1** and **2**, respectively (entries 13, 14), and pointing out a more remarkable promoting behavior of hydrochloric over nitric acid in these catalytic systems. In contrast to HNO_3, the use of HCl leads to the formation of cyclohexanol as the predominant product. This fact supports also the generation of cyclohexyl hydroperoxide as the primary product, whose presence was confirmed by following the

(23) (a) Kirillova, M. V.; Kirillov, A. M.; Kuznetsov, M. L.; Silva, J. A. L.; Fraústo da Silva, J. J. R.; Pombeiro, A. J. L. *Chem. Commun.* **2009**, 2353. (b) Kirillova, M. V.; Kirillov, A. M.; Pombeiro, A. J. L. *Adv. Synth. Catal.* **2009**, *351*, 2936. (c) Kirillova, M. V.; Kirillov, A. M.; Reis, P. M.; Silva, J. A. L.; Fraústo da Silva, J. J. R.; Pombeiro, A. J. L. *J. Catal.* **2007**, *248*, 130. (d) Kirillova, M. V.; Kirillov, A. M.; Pombeiro, A. J. L. *Chem.—Eur. J.* **2010**, *16*, 9485. (e) Kirillova, M. V.; Kuznetsov, M. L.; Reis, P. M.; da Silva, J. A. L.; Fraústo da Silva, J. J. R.; Pombeiro, A. J. L. *J. Am. Chem. Soc.* **2007**, *129*, 10531.

(24) (a) Schuchardt, U.; Cardoso, D.; Sercheli, R.; Pereira, R.; da Cruz, R. S.; Guerreiro, M. C.; Mandelli, D.; Spinace, E. V.; Pires, E. L. *Appl. Catal., A* **2001**, *211*, 1. (b) *Ullmann's Encyclopedia of Industrial Chemistry*, 6th ed; Wiley-VCH: Weinheim, 2002. (c) *Kirk-Othmer Encyclopedia of Chemical Technology*, 5th ed.; Wiley: Hoboken, NJ, 2004.

(25) (a) Kopylovich, M. N.; Kirillov, A. M.; Baev, A. K.; Pombeiro, A. J. L. *J. Mol. Catal. A: Chem.* **2003**, *206*, 163. (b) Fernandes, R. R.; Kirillova, M. V.; da Silva, J. A. L.; Fraústo da Silva, J. J. R.; Pombeiro, A. J. L. *Appl. Catal., A* **2009**, *353*, 107.

method (with PPh_3 addition) developed by Shul'pin et al.[15] Although not yet fully established, the role of an acid promoter can consist in its involvement in proton-transfer steps leading to the activation of the catalyst precursor through protonation of ligands with consequent unsaturation of the Cu^{II} centers, as well as in the enhancement of the oxidizing properties of H_2O_2 and hampering the eventual catalase activity.[9d,18a,22a]

Turnover numbers (TONs) up to 168 (for **1**) and 215 (for **2**) are also achieved (entries 13, 14) under typical reaction conditions, which can be further augmented to 315 and 467, respectively, when using an increased amount of cyclohexane and a more prolonged reaction time (entries 17, 18). The somewhat superior activity of **2** over **1** in almost all runs conceivably can be accounted for by the higher coordinative unsaturation of the copper centers in the former compound (i.e., five- vs six-coordinate Cu atoms in **2** and **1**, respectively),[8a] and by a closer Cu···Cu distance within the $[Cu_2(\mu\text{-}O)_2]^{2+}$ cores of **2** (Table 3). Although the detailed mechanistic study of the described catalysis lies outside of the scope of the present work, on the basis of prior background[8a,9d,18a,22] and of the experiments with radical traps that resulted in the suppression of the catalytic activity, we propose that the oxidation of cyclohexane proceeds via a free-radical mechanism, involving also the formation of cyclohexyl hydroperoxide (see above) as the primary oxidation product. Further metal-assisted decompositions of this organo hydroperoxide[15,22a] lead to the final products (cyclohexanol and cyclohexanone).

It is worthwhile to note that the activity levels of **1** and **2** achieved in the present work are superior to those exhibited by a variety of iron containing catalysts in the mild peroxidative oxidation of cyclohexane.[25,26] Furthermore, **1** and **2** are used in a 10-fold lower amount than that typically required by many state-of-the-art catalytic systems,[8a,9c,9d,18a,22,25] thus allowing to achieve a rather high catalytic efficiency with TONs up to about 470. These TONs are superior to those previously reported for the mild oxidation of cyclohexane employing other very efficient iron containing catalyst precursors, namely, bearing a heterotrimetallic[22d] $Fe^{III}/Cu^{II}/Co^{III}$ or hexairon(III)[27] core.

Conclusions

In the present study, we have developed a new convenient route to heterometallic Cu^{II}/Fe^{II} 3D coordination polymers, based on the aqueous-medium self-assembly of the $[Cu_2(\mu\text{-aminopolyalcoholate})_2]^{2+}$ nodes and the octahedral $[Fe(CN)_6]^{4-}$ linkers. This synthetic approach broadens the generality of our previously reported self-assembly method,[9] namely, by allowing an easy single-step generation of *heterometallic* Cu/Fe coordination networks, which proceeds in aqueous medium, under ambient conditions and using simple and cheap commercially available chemicals.

We have also shown that a slight modification of the aminopolyalcohol (main ligand source) from triethanolamine to *N*-methyldiethanolamine affects the resulting 3D networks of the coordination polymers **1** and **2**. Their crystal structures feature either regular (**1**) or distorted (**2**) octahedral net skeletons, based respectively on linear or wave-like ~Fe-CN-$Cu_2(\mu\text{-}O)_2$-NC-Fe-CN-$Cu_2(\mu\text{-}O)_2$~ cross-linking motifs. Besides, these compounds represent the first examples[3] of heterometallic Cu/Fe coordination polymers constructed from the $[Cu_2(\mu\text{-aminopolyalcoholate})_2]^{2+}$ nodes and the hexacyanoferrate linkers. An interesting feature of compounds **1** and **2** also concerns the reversible escape and binding processes toward water and methanol molecules.

The magnetic study reveals that compounds **1** and **2** follow the Heisenberg dinuclear model and fit the general trend for the alkoxo-bridged copper(II) complexes, displaying antiferromagnetic couplings for large Cu−O−Cu bridging angles and ferromagnetic couplings for angles smaller than 98°. A weak magnetic coupling through the $[Fe(CN)_6]^{4-}$ group is observed in **2**, but the strong intra-dimer antiferromagnetic coupling hampers its detection in **1**. These compounds also illustrate the versatility of the $[Cu_2(\mu\text{-}O)_2]^{2+}$ cores that may exhibit quite different structural features, thus resulting in very distinct magnetic behaviors.

In addition, the work extends the still limited application of heterometallic coordination polymers in catalysis,[11] representing also the first example of cyclohexane oxidation catalyzed by a heterometallic Cu/Fe coordination polymer. Hence, **1** and **2** are capable of catalyzing the mild peroxidative oxidation of cyclohexane to cyclohexanol and cyclohexanone, by aqueous H_2O_2 in acetonitrile medium at 25 °C, and in the presence of an acid promoter (homogeneous catalytic system). Compound **2** appears to show a higher level of activity, with maximum total yields (based on cyclohexane) and TONs up to about 22% and 470, respectively.

Exploration of the present self-assembly approach will be pursued for the design of novel metal−organic frameworks, namely, by utilizing other cyanometallate linkers and various Cu-aminopolyalcoholate nodes.

Acknowledgment. This work has been partially supported by the Foundation for Science and Technology (FCT), Portugal, its PPCDT (FEDER funded) and "Science 2007" programs. J.S. acknowledges the Servicio General de Medidas Magnéticas of the Universidad de La Laguna for the magnetic measurement facilities.

Supporting Information Available: Additional structural representations (Figures S1, S2), plots of differential thermal analyses (Figure S3) and their summary (Table S11), and the crystallographic files in CIF format for compounds **1** and **2**. This material is available free of charge via the Internet at http://pubs.acs.org.

(26) (a) Shilov, A. E.; Shul'pin, G. B. *Activation and Catalytic Reactions of Saturated Hydrocarbons in the Presence of Metal Complexes*; Kluwer Academic Publishers: Dordrecht, The Netherlands, 2000. (b) Nizova, G. V.; Krebs, B.; Süss-Fink, G.; Schindler, S.; Westerheide, L.; Cuervo, L. G.; Shul'pin, G. B. *Tetrahedron* **2002**, *58*, 9231. (c) Shul'pin, G. B.; Nizova, G. V.; Kozlov, Y. N.; Cuervo, L. G.; Süss-Fink, G. *Adv. Synth. Catal.* **2004**, *346*, 317. (d) England, J.; Britovsek, G. J. P.; Rabadia, N.; White, A. J. P. *Inorg. Chem.* **2007**, *46*, 3752. (e) Romakh, V. B.; Therrien, B.; Süss-Fink, G.; Shul'pin, G. B. *Inorg. Chem.* **2007**, *46*, 3166. (f) Silva, T. F. S.; Alegria, E. C. B. A.; Martins, L. M. D. R. S.; Pombeiro, A. J. L. *Adv. Synth. Catal.* **2008**, *350*, 706. (g) Tanase, S.; Marques-Gallego, P.; Browne, W. R.; Hage, R.; Bouwman, E.; Feringa, B. L.; Reedijk, J. *Dalton Trans.* **2008**, 2026. (h) England, J.; Gondhia, R.; Bigorra-Lopez, L.; Petersen, A. R.; White, A. J. P.; Britovsek, G. J. P. *Dalton Trans.* **2009**, 5319.

(27) Trettenhahn, G.; Nagl, M.; Neuwirth, N.; Arion, V. B.; Jary, W.; Pochlauer, P.; Schmid, W. *Angew. Chem., Int. Ed.* **2006**, *45*, 2794.